# Effect of Average Phospholipid Curvature on Supported Bilayer Formation on Glass by Vesicle Fusion

Chiho Hamai,* Tinglu Yang,† Sho Kataoka,† Paul S. Cremer,† and Siegfried M. Musser*
*Department of Molecular and Cellular Medicine, The Texas A&M University System Health Science Center, College Station, Texas 77843; and †Department of Chemistry, Texas A&M University, College Station, Texas 77842

ABSTRACT The adsorption of large unilamellar vesicles composed of various combinations of phosphatidylcholine, phosphatidylethanolamine (PE), monomethyl PE, and dimethyl PE (PE-$Me_2$) onto a glass surface was studied using fluorescence microscopy. The average lipid geometry within the vesicles, described mathematically by the average intrinsic curvature, $C_{0,ave}$, was methodically altered by changing the lipid ratios to determine the effect of intrinsic curvature on the ability of vesicles to rupture and form a supported lipid bilayer. We show that the ability of vesicles to create fluid planar bilayers is dependent on $C_{0,ave}$ and independent of the identity of the component lipids. When the $C_{0,ave}$ was $\sim -0.1$ nm$^{-1}$, the vesicles readily formed supported lipid bilayers with almost full mobility. In contrast, when the $C_{0,ave}$ ranged from $\sim -0.2$ to $\sim -0.3$ nm$^{-1}$, the adsorbed vesicles remained intact upon the surface. The results indicate that the average shape of lipid molecules within a vesicle ($C_{0,ave}$) is essential for determining kinetically viable reactions that are responsible for global geometric changes.

## INTRODUCTION

Phospholipid vesicles spontaneously adsorb to solid surfaces, sometimes rupturing and fusing to form a supported lipid bilayer (SLB) (1–10). These SLBs are useful biomimetic systems for elucidating intrinsic properties of biological membranes, including the functions of membrane proteins, by means of a number of surface analytical techniques. To serve as an appropriate biological membrane mimic, the model lipid bilayer must have a lipid composition resembling the archetypical membrane. Indeed, specific lipids are essential for maintaining the function of some membrane proteins (11,12). The properties of phosphatidylcholine (PC) vesicles, their fusogenicity with surfaces, and the characteristics of PC SLBs are well studied (1–8). However, the phospholipid composition of certain biological membranes, for example, the *Escherichia coli* cytoplasmic membrane, can be as high as 70–80% phosphatidylethanolamine (PE) (12,13). Thus, to study the properties of such bacterial membranes, or the proteins within them, in an SLB system, it is necessary to understand the different physical properties introduced by the different chemical structures of the major component lipids. Therefore, we have examined the fusogenicity of PE-containing vesicles with a glass surface.

The difference between PEs and PCs is that the latter contain three methyl groups on the headgroup nitrogen, whereas the former contain protons. This difference in chemical structure gives rise to differences in hydration, hydrogen bonding, and pH-dependent charge as well as a geometrical difference; the headgroup of PE is smaller, such that the width of the PE headgroup is less than that of the hydrophobic tail (Fig. 1). Herein, we are primarily concerned with the geometrical difference.

There are several models that describe the properties of lipid systems consisting of conformationally flexible lipid monomers in a quantitative manner (14), one of which is the model formulated by Gruner for an inverted monolayer of hexagonal phases and later extended to monolayers with arbitrary shapes (15,16). Due to its small headgroup, PE prefers to form a hexagonal phase (Fig. 1) at room temperature. In Gruner's model, the free energy per unit area in the lipid monolayer of the hexagonal phase ($F_H$) is approximated by

$$F_H = \frac{1}{2}\kappa\left(\frac{1}{R} - \frac{1}{R_0}\right)^2 = \frac{1}{2}\kappa(C - C_0)^2,$$

where $\kappa$ is the bending modulus for the monolayer, $R$ is the radius of a pivotal plane where the surface area of a lipid remains constant, and $R_0$ is the radius of intrinsic curvature describing the lipid assembly in a stress-free state with the minimum energy. The pivotal plane lies close to the boundary between the hydrocarbon and polar group layers (17). $R_0$ is experimentally measured as the radius of the inverted micellar structure (hexagonal phase) in water containing alkanes such as tetradecane (18). The intrinsic curvature, $C_0 = 1/R_0$, is a more convenient mathematical formulation that avoids the singularity at $R_0 = \pm\infty$ for which $C_0$ is simply 0 (lamellar phase). By convention, the signs of $C$ and $C_0$ are negative for the hexagonal phase and are positive when the lipid monolayer is curled in the opposite direction.

The mechanism of SLB formation has been examined for PC vesicles using a quartz crystal microbalance equipped with dissipation monitoring (QCM-D), surface plasmon resonance, fluorescence microscopy, and atomic force microscopy (AFM) (3–8). The current model is that the vesicles first adsorb and flatten due to favorable interactions with the

*Submitted June 28, 2005, and accepted for publication October 28, 2005.*

Address reprint requests to Siegfried M. Musser, Tel.: 979-862-4128; Fax: 979-847-9481; E-mail: smusser@tamu.edu.



0006-3495/06/02/1241/08 $2.00

doi: 10.1529/biophysj.105.069435

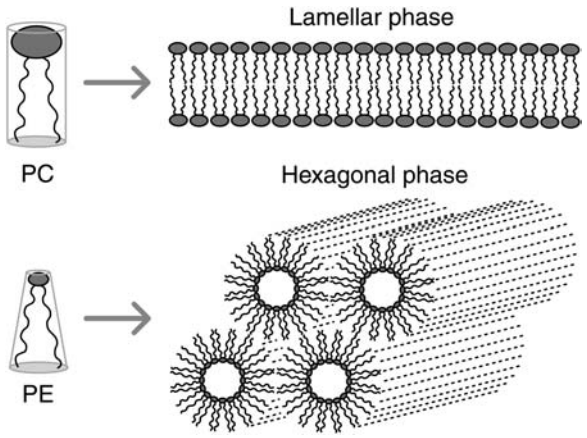


FIGURE 1 Lamellar and hexagonal phases. The top and bottom illustrations show the energetically preferred structures for lipids with $C_0 \sim 0$ (e.g., PC) and $C_0 < 0$ (e.g., PE), respectively. Adapted from Israelachvilli (44).

surface, then possibly fuse together forming larger vesicles (depending on the surface and vesicle composition) (3,7,19), and finally rupture and fuse to form SLBs. Since the deformation, fusion, and rupture events involve membrane surfaces of different curvatures, we anticipated that a bilayer's intrinsic curvature might affect at least one of these events.

In this work, we have focused on a functional consequence of the geometrical differences between PE and PC with respect to SLB formation on a glass surface. We used large unilamellar vesicles (LUVs) that were composed of PC and various forms of PE and altered the average intrinsic curvature of the component lipids by changing the PC/PE ratio. Here we report that the average geometric structure of the component lipids affects vesicle fusion.

## MATERIALS AND METHODS

### Materials

1,2-Dioleoyl-*sn*-glycero-3-phosphocholine (DOPC), 1,2-dioleoyl-*sn*-glycero-3-phosphoethanolamine (DOPE), 1,2-dioleoyl-*sn*-glycero-3-phosphoethanolamine-*N*-methyl (DOPE-Me), 1,2-dioleoyl-*sn*-glycero-3-phosphoethanolamine-*N*,*N*-dimethyl (DOPE-$Me_2$), and 1-oleoyl-2-hydroxy-*sn*-glycero-3-phosphocholine (Lyso-PC) were purchased from Avanti Polar Lipids (Alabaster, AL). Texas Red 1,2-dihexadecanoyl-*sn*-glycero-3-phosphoethanolamine, triethylammonium salt (TR-DHPE), *N*-(7-nitrobenz-2-oxa-1,3-diazol-4-yl)-1,2-dihexadecanoyl-*sn*-glycero-3-phosphoethanolamine, triethylammonium salt (NBD-PE), and 5-(and-6)-carboxyfluorescein mixed isomers (CF) were purchased from Molecular Probes (Eugene, OR). All the lipids were used as received. 7X detergent (No. 76-670-93, MP Biomedicals, Aurora, OH) was used to clean glass slides. The buffer used for all experiments was 200 mM KCl, 50 mM HEPES-KOH, pH 8.0. The unsaturated lipids used here have gel to lamellar phase transition temperatures below 0°C (20), and thus, the lipid bilayers are completely fluid in our room temperature experiments. These unsaturated lipids were chosen intentionally since bilayers consisting exclusively of these lipids should not form lipid rafts (21).

### Preparation of large unilamellar vesicles

LUVs were prepared as follows. Phospholipids were mixed in chloroform at the desired compositions. As a fluorescent marker, TR-DHPE or NBD-PE was added to all lipid preparations. When the effect of TR-DHPE or NBD-PE concentration was examined (see Fig. 6), 0.5, 1.0, or 2.0 mol % of the dye-labeled lipid was added. For all other lipid preparations, 0.5 mol % TR-DHPE was added. Bulk chloroform was removed under a stream of nitrogen; any remaining solvent was evaporated under house vacuum for 1 h. Buffer was then added to the dried phospholipid to yield a total lipid concentration of ~0.7 mM. After lipid hydration, the samples were subjected to ≥7 freeze-thaw cycles (liquid nitrogen/room temperature) and were then extruded 10 times through two stacked polycarbonate membrane filters with a pore size of 100 nm using a LIPEX extruder (Northern Lipids, Vancouver, BC, Canada). Particle size distributions were determined by dynamic light scattering (90 Plus Particle Sizer, Brookhaven Instruments Corporation, Holtsville, NY) for all lipid compositions before use. A dominant peak was typically observed indicating the presence of ~90–180 nm-sized particles (size depended on lipid composition). Phospholipid compositions are expressed as mole ratios within the nonfluorescent lipids: e.g., DOPC/DOPE (5:5) denotes a lipid composition of 49.25% DOPC, 49.25% DOPE, and 0.5% TR-DHPE. Since lipid compositions were varied in units of 10 mol %, lipid mole ratios are quoted such that the numbers total to 10 to allow easier mental conversion to approximate percentages: e.g., (5:5) and (4:6) rather than the mathematically simplified (1:1) and (2:3), respectively.

### Fluorescent dye in the vesicle lumen

To incorporate CF into the vesicle lumen (inside aqueous compartment), LUVs were formed in the presence of 0.5 mM CF. External dye molecules were removed by dialysis (60 kDa molecular weight cutoff) against 1250 volumes of buffer for 1 h at 4°C. The dialysate was then exchanged, and the dialysis was continued for another 2 h at 4°C. Absorption measurements at 492 nm indicated that ~99.5% of the dye was removed. Assuming an area of 70 $Å^2$ occupied by a lipid molecule in LUVs (22), ~0.25% of the initial amount of CF was entrapped in the LUVs; therefore, ~0.25% remained outside the LUVs.

### Formation of supported bilayers

Glass coverslips (22 × 22 mm, No. 1, VWR Scientific, West Chester, PA) were soaked for 20 min in a 7X detergent/water (1:3) solution, which was heated to clarity. After rinsing with a copious amount of purified water, the coverslips were dried under a stream of nitrogen, baked at 440°C for 5 h, and cooled to room temperature. Coverslips were used within 24 h after cleaning. Lipid solutions were deposited onto the coverslip surface in poly(dimethylsiloxane) chambers (attached to the coverslips through light pressure) and incubated for 10 min at room temperature. The surface was then rinsed by copious amounts of buffer to remove nonadsorbed lipids.

### Fluorescence recovery after photobleaching measurements

Fluorescence recovery after photobleaching (FRAP) experiments (23,24) were performed using a Zeiss Axiovert (Jena, Germany) 200 M fluorescence microscope. TR-DHPE, NBD-PE, and CF were photobleached (46 $\mu$m diameter spot) with a 568 nm (2 mW; TR-DHPE) or 488 nm (1 mW; NBD-PE and CF) laser beam (Spectra-Physics, Mountain View, CA) Stabilite 2018-RM). Laser power was measured at the specimen plane. Fluorescence recovery was recorded at 10× magnification. The fraction of mobile dye molecules ($F$) was obtained from the FRAP data according to the following relation:

$$F = \frac{I_\infty - I_0}{I_i - I_0},$$

where $I_i$, $I_0$, and $I_\infty$ are the total fluorescence intensities within the photobleached area before the bleaching pulse, immediately after the bleaching pulse, and after recovery (stable signal), respectively. Phospholipids within an SLB are expected to be free to diffuse within a large planar area of at least tens of micrometers and therefore were considered to constitute the ''mobile'' fraction. In contrast, the phospholipids in vesicles that bind to the surface but do not fuse to form an SLB are expected to be restricted to diffuse within single nanometer-scale vesicles and therefore were considered to constitute the ''immobile'' fraction. Therefore, a value of $F = 1$ and a homogeneous fluorescence intensity pattern were taken to imply that 100% of the photobleached dye molecules are attached to lipid molecules free to diffuse within the sample plane. As a point of reference, the diffusion constant obtained for DOPC bilayers obtained under these conditions was 2.1 ± 0.1 $\mu m^2/s$.

### Estimation of the average intrinsic curvature

The average intrinsic curvature for lipid mixtures, $C_{0,ave}$, was approximated as follows:

$$C_{0,ave} = \sum_j X_j C_{0,j},$$

where $X_j$ and $C_{0,j}$ are the mole fraction and the intrinsic curvature for each component lipid, respectively (25). Since a value for $C_{0,TR\text{-}DHPE}$ is not available, we approximated the average intrinsic curvature value by not including the contribution of TR-DHPE (0.5 mol %), i.e., $C'_{0,ave} = C_{0,ave} - 0.005C_{0,TR\text{-}DHPE}$. The consequence of this approximation is that all the abscissa values in Fig. 5 are offset by the same unknown (but small) amount.

## RESULTS

### PE inhibits SLB formation

The chemical structures of the lipids used in this study are shown in Fig. 2 *A*. Since the $pK_a$ of the primary amine in PE is ~11 (26), the nitrogen in PE is virtually always protonated at pH 8. Therefore, at pH 8, the lipids in Fig. 2 *A* are all zwitterionic with zero net charge. In addition, each hydrophobic chain has the identical chemical structure. Hence, under our experimental conditions, the chemical structures of the lipids used differ from one another only in the size of the polar headgroups relative to that of the hydrophobic tail: Lyso-PC is cone shaped, DOPC is cylindrical, and DOPE is inverted-cone shaped (Fig. 2 *A*). These geometrical differences are described mathematically by the intrinsic curvature, $C_0$. The $C_0$ values for DOPC, DOPE-Me, and DOPE are known to be linearly proportional to the number of methyl groups on the headgroup nitrogen (25,27). The value for DOPE-$Me_2$ is not available, but can be predicted by extrapolation (Fig. 2 *B*).

PC vesicles readily fuse to form an SLB on glass (2–8). To examine the role of lipid shape on vesicle fusion, we methodically decreased the percentage of PC in LUVs and concomitantly increased the percentage of some form of PE lipid. After incubating the LUVs with glass coverslips for 10 min, the mobile fraction was determined from the FRAP of TR-DHPE, a fluorescent marker lipid (Materials and Methods). For all the PE variants used, the mobile fractions varied from ~1 to 0 depending upon the PC/PE ratio (Fig. 3). When the vesicles contained no PE, fluid bilayers were obtained. However, as the PE mole ratio in the LUVs reached 20–60%, lipid mobility on the coverslip surface dropped to zero. It should be noted that a maximum of 50 mol % DOPE was used for the experiments described in Fig. 3 *A* since the lamellar to hexagonal phase transition in DOPC:DOPE vesicles occurs by 60% DOPE (28,29). In contrast, pure DOPE-Me and DOPE-$Me_2$ form lamellar phases at room temperature (20,30,31).

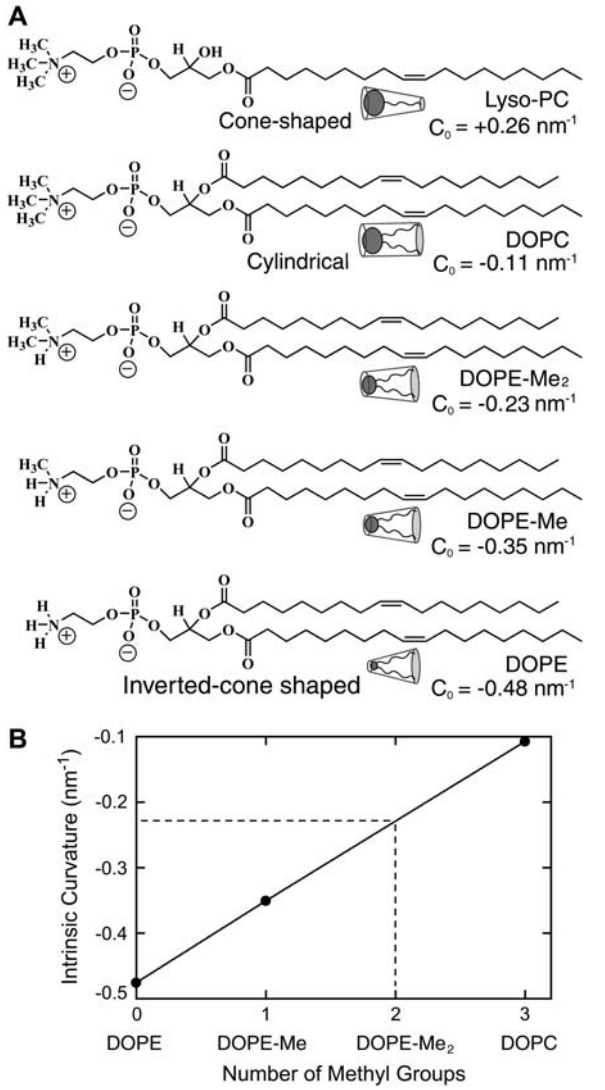


FIGURE 2 Summary of lipid characteristics. (*A*) Chemical structures, geometric shapes, and intrinsic curvature ($C_0$) for the lipids used in this study. (*B*) Estimation of the $C_0$ for DOPE-$Me_2$. The literature values for $C_{0,DOPE}$, $C_{0,DOPE\text{-}Me}$, and $C_{0,DOPC}$ (25,27) predict a $C_0$ of $-0.23\ nm^{-1}$ for DOPE-$Me_2$, assuming a linear relationship between the number of the methyl groups on the headgroup nitrogen and the $C_0$.

### High PE ratios

Although lipids in DOPC:DOPE solutions in which >50 mol % of the lipid is DOPE are thermodynamically favored

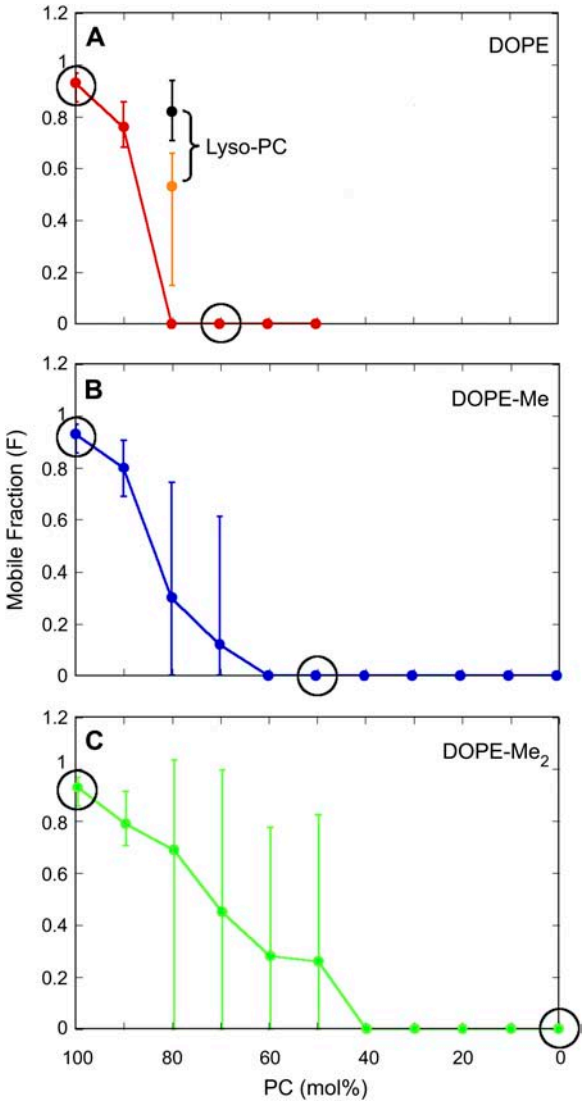


FIGURE 3 Mobile fraction dependence on the PC/PE mole ratio. (*A*) The mobile fraction determined after LUVs with different DOPC/DOPE molar ratios (*red*) were adsorbed onto a glass coverslip. The $C_{0,ave}$ of DOPC/DOPE (8:2) LUVs was increased by exchanging Lyso-PC for DOPC to yield DOPC/Lyso-PC/DOPE ratios of 7:1:2 (*orange*) and 6:2:2 (*black*). (*B*) Same as *A* but for different DOPC/DOPE-Me molar ratios. (*C*) Same as *A* but for different DOPC/DOPE-$Me_2$ molar ratios. All the LUVs were labeled with 0.5 mol % TR-DHPE. Since the mobile fraction determinations were not normally distributed about a mean (values $>1$ and $<0$ are theoretically impossible), bars show the maximum and minimum for each measurement; points are the mean of 5–17 determinations (different areas on 2–6 bilayer samples). The distribution of mobile fractions determined for LUVs with lipid ratios in the transition region between high and low mobility appeared bimodal with most values ~0 or ~0.5–1; values between 0 and 0.5 were rarely obtained. Circled points show the lipid compositions that were used in the CF experiments.

to form the hexagonal phase, we did examine such mixtures directly since they are more appropriate mimics of bacterial cytoplasmic membranes than those with higher PC content. Lipid mixtures with such high DOPE ratios were extruded through polycarbonate membrane filters with a 100 nm pore size and then deposited onto a glass surface. Relatively high mobile fractions were obtained for DOPC/DOPE (4:6) and (3:7) lipid mixtures (0.79 and 0.74, respectively). At 100× magnification, inhomogeneous fluorescence patterns were observed with at least four distinguishable features: bright spots, fiber-like structures, and dark and light domains (Fig. 4 *A*). These data are inconsistent with the presence of a pure SLB. In control experiments, a homogeneous fluorescence intensity (''homogeneous to the diffraction limit''; the theoretical diffraction limit was ~260 nm based on the conditions of the experiments) was observed for DOPC vesicles, consistent with the presence of an SLB (Fig. 4 *B*). For comparison, an image of the immobile structure obtained

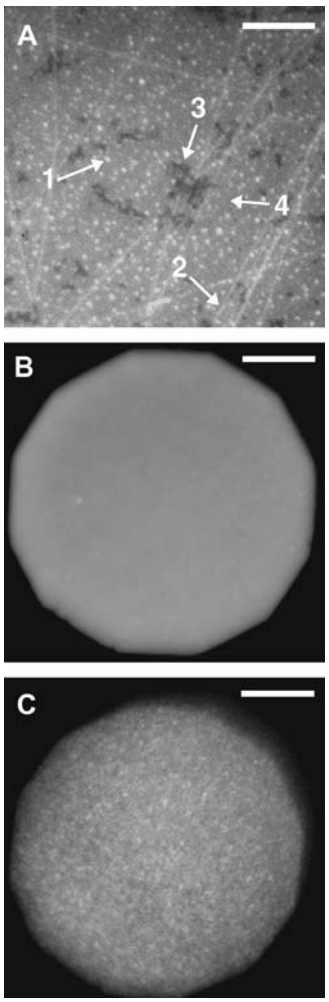


FIGURE 4 High magnification images of the adsorbed structures observed for LUVs of various lipid compositions. Fluorescence images obtained 10 min after adsorption of (*A*) DOPC/DOPE (4:6), (*B*) DOPC, and (C) DOPC/DOPE-$Me_2$ (1:9) lipid mixtures. Bright spots, fiber-like structures, and dark and light domains are marked in *A* by arrows with the numbers 1, 2, 3, and 4, respectively. The concentration of TR-DHPE is 0.5 mol % for all the samples. The illumination aperture sharply imaged at some edges (*black*) illustrates that the glass surface is in focus; this internal control is unnecessary when an obviously inhomogeneous surface structure is present. Scale bars, 10 $\mu$m. Magnification, 100×.

from DOPC/DOPE-$Me_2$ (1:9) LUVs is also shown (Fig. 4 *C*). These results are consistent with formation of the thermodynamically favored hexagonal phase at high PE ratios and indicate that high mobility does not necessarily imply a pure SLB.

## Role of the average intrinsic curvature

We reasoned that the shape change introduced by the geometrical differences between PC and PE lipids might explain why lipid mobility after LUV adsorption to glass is inhibited by PE lipids. To more directly address this issue, the data in Fig. 3 were replotted as a function of the average intrinsic curvature, $C'_{0,ave}$ (Fig. 5, *red*, *blue*, and *green*). The data suggested that LUVs with a $C'_{0,ave} \approx -0.1$ nm$^{-1}$ will form a structure with high lipid mobility and those with a $C'_{0,ave}$ of $-0.2$ to $-0.3$ nm$^{-1}$ will not; as the $C'_{0,ave}$ decreases from $\sim -0.1$ to $\sim -0.2$ nm$^{-1}$, the average lipid mobility will progressively decrease.

The predictive nature of this conclusion was first tested by replacing some of the PC in a DOPC/DOPE (8:2) mixture with Lyso-PC without changing the amount of DOPE to increase the $C'_{0,ave}$ as a means to recover lipid mobility. The lipid mobility was indeed recovered for LUVs with DOPC/Lyso-PC/DOPE ratios of 7:1:2 and 6:2:2 (Fig. 3 *A*, *orange* and *black*, respectively). When the lipid ratios within DOPC/Lyso-PC/DOPE LUVs were varied, the mobile fraction was well predicted by $C'_{0,ave}$ according to the relationship established from the two-component mixtures (Fig. 5, *black*).

As a second test of the predictive power of $C_{0,ave}$, we raised the concentration of TR-DHPE or NBD-PE from 0.5 to 1 and 2 mol % in a DOPC/DOPE (7:3) mixture. We reasoned that the large aromatic group bound to the PE headgroup in these fluorescent lipids would increase the mobile fraction by increasing the $C_{0,ave}$ in a manner similar to Lyso-PC. As expected, lipid mobility was regained at elevated levels of TR-DHPE and NBD-PE (Fig. 6). Under these conditions, the presumably increased $C_{0,ave}$ clearly dominates over the known ability of negatively charged, dye-labeled lipids to inhibit vesicle fusion by electrostatic repulsion (2). Since experiments were not performed to distill the role of these two variables (average lipid geometry and electrostatics) on the mobile fraction obtained from TR-DHPE- or NBD-PE-containing LUVs, it is inappropriate to estimate a $C_0$ for TR-DHPE and NBD-PE from the current data. Nonetheless, higher TR-DHPE and NBD-PE concentrations (but still only a few mole percent) in DOPC/DOPE (7:3) LUVs promote the formation of a mobile lipid phase after vesicle adsorption to glass, consistent with the expectation that TR-DHPE and NBD-PE have (fairly large) positive intrinsic curvatures.

## ''Immobile'' lipids are in intact vesicles

Prior QCM-D studies have demonstrated that EggPC vesicles adsorb but do not rupture on oxidized Au, oxidized Pt, and $TiO_2$ surfaces (4,6,7). Therefore, we suspected that the ''immobile'' lipids observed when low $C_{0,ave}$ LUVs were used meant that the vesicles did not rupture upon adhesion and, consequently, that the lipid molecules were confined within their adsorbed structures. To verify vesicle adsorption without rupture, vesicles encapsulating CF were deposited on the surface. Vesicles that fused resulting in an SLB were expected to lose their lumenal CF and therefore yield a low CF signal; those that adsorbed but did not fuse were expected to retain their lumenal CF and therefore yield a high CF signal. The loss of CF intensity upon vesicle

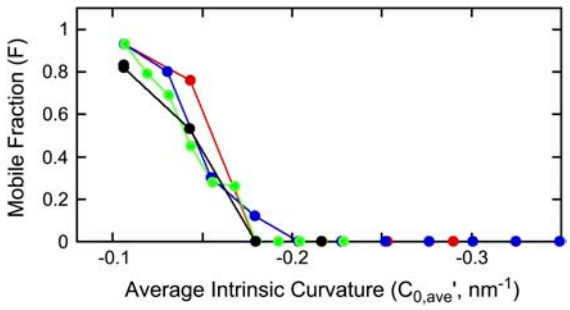


FIGURE 5 Mobile fraction dependence on the average intrinsic curvature. Mobile fractions for the lipid compositions in Fig. 3 based on calculated $C'_{0,ave}$ values: DOPC/DOPE (*red*), DOPC/DOPE-Me (*blue*), and DOPC/DOPE-$Me_2$ (*green*). The $C'_{0,ave}$ values of $-0.22$, $-0.18$, $-0.18$, $-0.14$, $-0.11$, and $-0.11$ nm$^{-1}$ were calculated from DOPC/Lyso-PC/DOPE ratios of 5:1:4, 6:3:1, 4:2:4, 7:1:2, 6:2:2, and 8:1:1, respectively (*black*). Only mean values are shown; maximum and minimum values are omitted for clarity. Note that the $C_0$ for TR-DHPE is not known; consequently, the average intrinsic curvature was estimated without this contribution as $C'_{0,ave}$ (Materials and Methods). The correction introduced by a $C_{0,ave}$ estimate that explicitly includes the TR-DHPE contribution (0.5 mol % in all cases) would simply be addition of the same constant to all abscissa values.

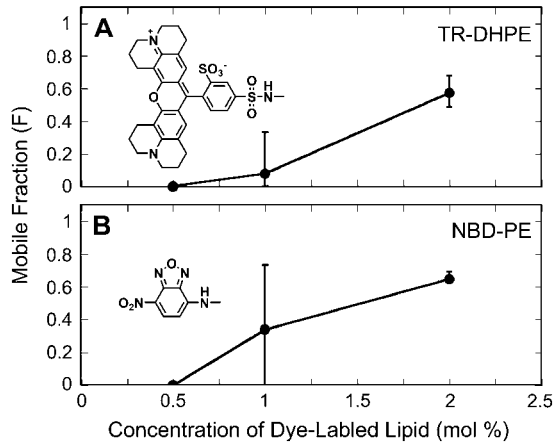


FIGURE 6 Mobile fraction dependence on TR-DHPE or NBD-PE concentration. The mobile fraction was determined for increasing amounts of TR-DHPE (*A*) and NBD-PE (*B*) in DOPC/DOPE (7:3) vesicles. Chemical structures of the dye molecules attached to the PE headgroups are also shown. Points are the mean of eight determinations (different areas on two bilayer samples); bars show the maximum and minimum for each measurement.

rupture has been recently monitored in total internal reflection fluorescence studies (3). In addition, lumenal CF has been widely used to report membrane fusion events (32). DOPC, DOPC/DOPE (7:3), DOPC/DOPE-Me (5:5), and DOPE-$Me_2$ were chosen as representative lipid compositions (marked by *circles* in Fig. 3), and LUVs were constructed that encapsulated CF. In addition, all of these LUVs were labeled with 0.5 mol% TR-DHPE to report on lipid mobility. For these four lipid compositions, no differences in the extent of lipid mobility were observed between samples that contained CF (not shown) and those that did not (Fig. 3). The very low CF fluorescence intensity observed for DOPC vesicles after a 10 min incubation period with a glass coverslip indicates that the CF molecules were thoroughly washed away, and therefore that the vesicles ruptured. In contrast, the intense CF emission observed for the other three samples suggests that the vesicles adsorbed but did not (fully) rupture (Fig. 7). FRAP experiments on the CF within the immobile lipid samples indicated that CF also is immobile, consistent with the notion that the dye remained trapped within the vesicle lumen. Although each of the immobile samples yielded high CF fluorescence intensities, the mean of these intensities varied by as much as ~28%. It is conceivable that some vesicles may have lost their CF content due to rupture. AFM images were obtained to test this hypothesis. These AFM data do not support the rupture of such a significant percentage of the vesicles in the immobile samples (data not shown). Different vesicle size distributions, different adsorption efficiencies, and/or different amounts of CF within the vesicles are likely sufficient to explain the variability of CF intensities within adsorbed intact vesicles. Despite the fact that CF is water soluble, it clearly influences vesicle structural stability since high CF concentrations lead to vesicle instability.

## DISCUSSION

The major conclusion of this study is that the average geometry of the lipids in LUVs has a dramatic effect on the ability of vesicles to form an SLB on a glass surface. Previous studies using PC vesicles have suggested the following sequence of events when vesicles interact with a glass or $SiO_2$ surface: adsorption, deformation/flattening due to favorable van der Waals interactions with the surface, and rupture to form an SLB (Fig. 8) (3–8). Our results demonstrate that between $C'_{0,ave} = -0.1$ $nm^{-1}$ and $-0.2$ $nm^{-1}$, there is a dramatic shift in the ability of LUVs to form an SLB. At higher values of $C_{0,ave}{}'$ (i.e., high PC ratios), LUVs readily form SLBs. In contrast, at lower $C_{0,ave}{}'$ values (i.e., high PE ratios), pure SLBs are never formed. Thus, the $C_{0,ave}$ is an important parameter influencing whether vesicle rupture occurs.

The structural difference between PC and PE headgroups introduces different chemical functional properties in addition to the overall geometrical difference of the lipids as described by $C_0$. We already discussed the potential for charge differences depending on pH. Our experiments were conducted at pH 8, well below PE's $pK_a$ of ~11; thus, PC and PE have identical charges under our conditions. Hydration and hydrogen bonding capabilities are also different for PC and PE due to the fundamentally different interactions of the N-H and N-$CH_3$ moieties on the headgroup nitrogen with the surrounding water. PC is typically more hydrated than PE because of its larger size (33). However, since monomethyl PE has similar hydration properties as PC (34), it seems

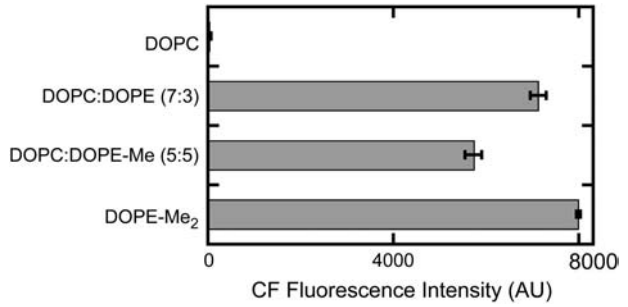


FIGURE 7 Lumenal CF fluorescence intensity after vesicle adsorption for representative lipid compositions. The lumenal CF intensity for vesicles with four representative lipid compositions (*circled points* in Fig. 3) after a 10 min incubation period with glass coverslips is indicated. Values (± SE) are the average of 5–20 determinations (different areas on 1–4 bilayer samples).

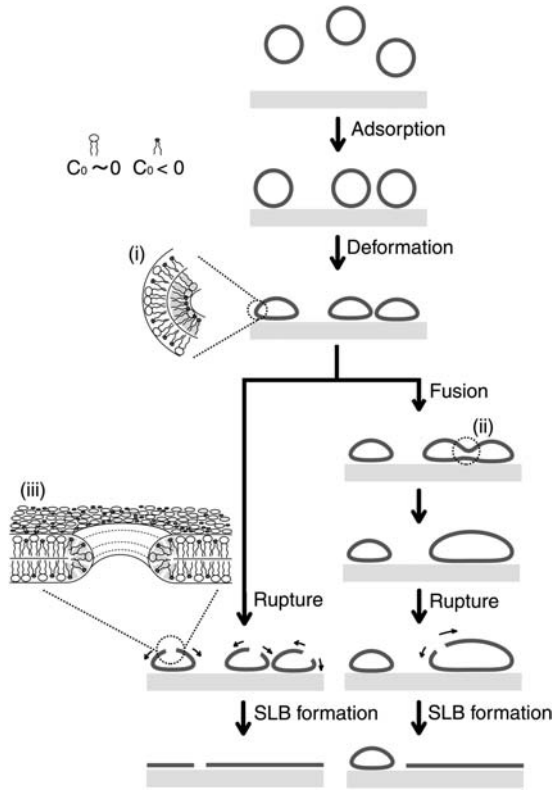


FIGURE 8 Possible mechanisms of supported bilayer formation. Vesicles adsorb, deform, and rupture to form an SLB. Under some conditions, vesicle-vesicle fusion occurs as an intermediate preceding vesicle rupture. See text for details.

unlikely that hydration alone explains the different behaviors of DOPC, DOPE-Me, and DOPE-$Me_2$ LUVs. The potential for PE to hydrogen bond with the glass surface suggests that vesicle interactions with the surface are stronger for PE vesicles. However, if hydrogen bonding interactions dominated the resulting LUV geometrical changes, PE would be expected to increase the capability of LUVs to form an SLB, not inhibit this process as we observed. Finally, DOPC/Lyso-PC/DOPE mixtures with the same headgroup compositions (i.e., DOPC/Lyso-PC/DOPE (8:0:2), (7:1:2), and (6:2:2); Fig. 3 *A*) provide different mobile fractions, arguing against differences in the hydrogen bonding capabilities of headgroup moieties as the dominant parameter controlling SLB formation. Instead, the overall geometry of the component lipids, described by $C_{0,ave}$ is the most reasonable explanation for our data.

There are at least two, possibly three, structural elements present during SLB formation from vesicles in which the $C_0$ of the component lipids could be critically important to the rate and efficiency of this process: i), the highly curved bilayer region introduced by the vesicle deformation that results from the vesicle's interaction with the surface; ii), the intermediate structures required for vesicle-vesicle fusion; and iii), the high positive curvature of the membrane edge surrounding the rupture pore (Fig. 8). Of these three structural elements, i and iii are generally agreed to be necessary for SLB formation. The importance of structure ii is still a matter of debate since it is unclear whether vesicle-vesicle fusion is required, or even a dominant pathway, for SLB formation on glass. It is clear that vesicle-vesicle fusion occurs on mica (19), but the surface plays a critical role in what happens after vesicle adsorption (6,7). On a glass surface, vesicle-vesicle fusion does occur if the vesicles contain high concentrations of fluorescent lipids (3). However, such vesicles are unstable and undergo isolated rupture with fairly high probability (3,8). As this study shows, high concentrations of dye-labeled lipids dramatically change the $C_{0,ave}$ and therefore may not report the behavior of vesicles devoid of these lipids.

We now consider more precisely how the $C_0$ of the component lipids might affect the formation and stability of the three structural motifs discussed above. Considering formation of structure i, the presence of negative curvature lipids (e.g., PE, PE-Me, and PE-$Me_2$) in the inner leaflet would be favored energetically, though their presence in the outer leaflet would be disfavored. The preference of PE for high curvature regions has been observed in mixed-lipid small unilamellar vesicles, where PE is found preferentially in the inner leaflet and PC in the outer leaflet (35). For an established vesicle to form structure i, we suspect that the lipid composition of the inner leaflet would provide the dominant contribution to the energy term since the radius describing the curvature is smaller; however, the total energy cost is not easy to estimate as the geometry of the adsorbed vesicle is unknown. It may, however, be small because the contribution from each leaflet is expected to be of opposite sign.

As discussed above, there is no compelling reason for us to postulate that vesicle-vesicle fusion (structure ii) precedes rupture in the experiments reported here. Nonetheless, it is formally possible, and if true, this process would likely be dependent on $C_{0,ave}$ due to the changes in bilayer curvature that necessarily accompany vesicular fusion events. Studies on vesicle-vesicle fusion in bulk solution have revealed that fusion is highly dependent on lipid geometry (36–41). However, the (nonbilayer) lipid structures associated with membrane fusion in bulk solution are stabilized by the presence of nonbilayer lipids (35,36,38,39,42). In contrast, we demonstrate here that SLB formation is inhibited by nonbilayer lipids, arguing against vesicle-vesicle fusion as a necessary intermediate step for SLB formation.

Finally, considering structure iii, it is expected that negative curvature lipids would be highly disfavored energetically at the edge of rupture pores. The most stable form of this domain structure seemingly requires partitioning of the available lipids with the largest $C_0$ values into the bilayer edge exposed to solution. Consistent with this hypothesis is a recent study, which examined the formation of pores within giant unilamellar vesicles, that revealed that cholesterol (which has a negative intrinsic curvature) destabilized a pore and made its lifetime much shorter, whereas detergents with positive intrinsic curvatures stabilized a pore and made its lifetime much longer (43). The tendency of high concentrations of dye-labeled lipid to induce isolated rupture (3,8) is also consistent with this hypothesis. An early event in SLB formation is possibly the rupture of a single vesicle to form a planar bilayer disk. The edge of such a bilayer disk would require high positive curvature lipids (as in a rupture pore) and would become more unfavorable when the concentration of negative curvature lipids in the bilayer were increased.

We therefore favor structure iii as the structure whose formation is most influenced by changes in lipid curvature.

We have demonstrated that the intrinsic curvature of a vesicle's component lipids contribute significantly to the events that occur after the vesicle interacts with a glass surface. Consequently, lipid shape is essential for determining the stability and feasibility of a number of poorly characterized transient substructures that govern SLB formation on glass.

This work was supported by the Program in Membrane Structure and Function, the National Institutes of Health (GM070622 for P.S.C.; GM065534 for S.M.M.), the Welch Foundation (A-1421 for P.S.C.; BE-1541 for S.M.M.), and the Mallinckrodt Foundation.

## REFERENCES

1. Brian, A. A., and H. M. McConnell. 1984. Allogeneic stimulation of cytotoxic T cells by supported planar membranes. *Proc. Natl. Acad. Sci. USA.* 81:6159–6163.

2. Cremer, P. S., and S. G. Boxer. 1999. Formation and spreading of lipid bilayers on planar glass supports. *J. Phys. Chem. B.* 103:2554–2559.
3. Johnson, J. M., T. Ha, S. Chu, and S. G. Boxer. 2002. Early steps of supported bilayer formation probed by single vesicle fluorescence assays. *Biophys. J.* 83:3371–3379.
4. Keller, C. A., and B. Kasemo. 1998. Surface specific kinetics of lipid vesicle adsorption measured with a quartz crystal microbalance. *Biophys. J.* 75:1397–1402.
5. Keller, C. A., K. Glasmästar, V. P. Zhdanov, and B. Kasemo. 2000. Formation of supported membranes from vesicles. *Phys. Rev. Lett.* 84:5443–5446.
6. Reimhult, E., F. Höök, and B. Kasemo. 2002. Vesicle adsorption on $SiO_2$ and $TiO_2$: dependence on vesicle size. *J. Chem. Phys.* 117:7401–7404.
7. Reimhult, E., F. Höök, and B. Kasemo. 2003. Intact vesicle adsorption and supported biomembrane formation from vesicles in solution: influence of surface chemistry, vesicle size, temperature, and osmotic pressure. *Langmuir.* 19:1681–1691.
8. Schönherr, H., J. M. Johnson, P. Lenz, C. W. Frank, and S. G. Boxer. 2004. Vesicle adsorption and lipid bilayer formation on glass studied by atomic force microscopy. *Langmuir.* 20:11600–11606.
9. Nollert, P., H. Kiefer, and F. Jahnig. 1995. Lipid vesicle adsorption versus formation of planar bilayers on solid surfaces. *Biophys. J.* 69: 1447–1455.
10. Puu, G., and I. Gustafson. 1997. Planar lipid bilayers on solid supports from liposomes: factors of importance for kinetics and stability. *Biochim. Biophys. Acta.* 1327:149–161.
11. van der Does, C., J. Swaving, W. van Klompenburg, and A. J. Driessen. 2000. Non-bilayer lipids stimulate the activity of the reconstituted bacterial protein translocase. *J. Biol. Chem.* 275:2472–2478.
12. Dowhan, W. 1997. Molecular basis for membrane phospholipid diversity: why are there so many lipids? *Annu. Rev. Biochem.* 66:199–232.
13. Morein, S., A. S. Andersson, L. Rilfors, and G. Lindblom. 1996. Wild-type *Escherichia coli* cells regulate the membrane lipid composition in a ''window'' between gel and non-lamellar structures. *J. Biol. Chem.* 271:6801–6809.
14. Kozlov, M. M., and D. Andelman. 1996. Theory and phenomenology of mixed amphiphilic aggregates. *Curr. Opin. Colloid In.* 1:362–366.
15. Gruner, S. M. 1985. Intrinsic curvature hypothesis for biomembrane lipid composition: a role for nonbilayer lipids. *Proc. Natl. Acad. Sci. USA.* 82:3665–3669.
16. Kozlov, M. M., S. L. Leikin, and V. S. Markin. 1989. Elastic properties of interfaces. Elasticity moduli and spontaneous geometric characteristics. *J. Chem. Soc.* 85:277–292.
17. Fuller, N., and R. P. Rand. 2001. The influence of lysolipids on the spontaneous curvature and bending elasticity of phospholipid membranes. *Biophys. J.* 81:243–254.
18. Rand, R. P., and V. A. Parsegian. 1997. Hydration, curvature, and bending elasticity of phospholipid monolayers. *In* Lipid Polymorphism and Membrane Properties. R. M. Epand, editor. Academic Press, San Diego, CA. 375–401.
19. Reviakine, I., and A. Brisson. 2000. Formation of supported phospholipid bilayers from unilamellar vesicles investigated by atomic force microscopy. *Langmuir.* 16:1806–1815.
20. Gruner, S. M., M. W. Tate, G. L. Kirk, P. T. C. So, D. C. Turner, D. T. Keane, C. P. S. Tilcock, and P. R. Cullis. 1988. X-ray diffraction study of the polymorphic behavior of N-methylated dioleoylphosphatidylethanolamine. *Biochemistry.* 27:2853–2866.
21. Mukherjee, S., and F. R. Maxfield. 2004. Membrane domains. *Annu. Rev. Cell Dev. Biol.* 20:839–866.
22. Gennis, R. B. 1989. Biomembranes: Molecular Structure and Function. Springer-Verlag, New York.
23. Axelrod, D., D. E. Koppel, J. Schlessinger, E. Elson, and W. W. Webb. 1976. Mobility measurement by analysis of fluorescence photobleaching recovery kinetics. *Biophys. J.* 16:1055–1069.
24. Soumpasis, D. M. 1983. Theoretical analysis of fluorescence photobleaching recovery experiments. *Biophys. J.* 41:95–97.
25. Keller, S. L., S. M. Bezrukov, S. M. Gruner, M. W. Tate, I. Vodyanoy, and V. A. Parsegian. 1993. Probability of alamethicin conductance states varies with nonlamellar tendency of bilayer phospholipids. *Biophys. J.* 65:23–27.
26. Cevc, G., A. Watts, and D. Marsh. 1981. Titration of the phase transition of phosphatidylserine bilayer membranes. Effects of pH, surface electrostatics, ion binding, and headgroup hydration. *Biochemistry.* 20:4955–4965.
27. Lewis, J. R., and D. S. Cafiso. 1999. Correlation between the free energy of a channel-forming voltage-gated peptide and the spontaneous curvature of bilayer lipids. *Biochemistry.* 38:5932–5938.
28. Rand, R. P., and N. L. Fuller. 1994. Structural dimensions and their changes in a reentrant hexagonal-lamellar transition of phospholipids. *Biophys. J.* 66:2127–2138.
29. Yang, L., L. Ding, and H. W. Huang. 2003. New phases of phospholipids and implications to the membrane fusion problem. *Biochemistry.* 42:6631–6635.
30. Siegel, D. P., and J. L. Banschbach. 1990. Lamellar/inverted cubic ($L_\alpha/Q_{II}$) phase transition in N-methylated dioleoylphosphatidylethanolamine. *Biochemistry.* 29:5975–5981.
31. Cherezov, V., D. P. Siegel, W. Shaw, S. W. Burgess, and M. Caffrey. 2003. The kinetics of non-lamellar phase formation in DOPE-Me: relevance to biomembrane fusion. *J. Membr. Biol.* 195:165–182.
32. Weinstein, J. N., R. Blumenthal, and R. D. Klausner. 1986. Carboxyfluorescein leakage assay for lipoprotein-liposome interaction. *Methods Enzymol.* 128:657–668.
33. McIntosh, T. J. 1996. Hydration properties of lamellar and nonlamellar phases of phosphatidylcholine and phosphatidylethanolamine. *Chem. Phys. Lipids.* 81:117–131.
34. Rand, R. P., N. Fuller, V. A. Parsegian, and D. C. Rau. 1988. Variation in hydration forces between neutral phospholipid bilayers: evidence for hydration attraction. *Biochemistry.* 27:7711–7722.
35. Yeagle, P. L. 1997. Membrane fusion intermediates. *In* Lipid Polymorphism and Membrane Properties. R. M. Epand, editor. Academic Press, San Diego, CA. 375–401.
36. Haque, M. E., and B. R. Lentz. 2004. Roles of curvature and hydrophobic interstice energy in fusion: studies of lipid perturbant effects. *Biochemistry.* 43:3507–3517.
37. Haque, M. E., T. J. McIntosh, and B. R. Lentz. 2001. Influence of lipid composition on physical properties and PEG-mediated fusion of curved and uncurved model membrane vesicles: ''nature's own'' fusogenic lipid bilayer. *Biochemistry.* 40:4340–4348.
38. Chernomordik, L. 1996. Non-bilayer lipids and biological fusion intermediates. *Chem. Phys. Lipids.* 81:203–213.
39. Chernomordik, L. V., S. S. Vogel, A. Sokoloff, H. O. Onaran, E. A. Leikina, and J. Zimmerberg. 1993. Lysolipids reversibly inhibit $Ca^{2+}$-, GTP- and pH-dependent fusion of biological membranes. *FEBS Lett.* 318:71–76.
40. Lee, J., and B. R. Lentz. 1997. Evolution of lipidic structures during model membrane fusion and the relation of this process to cell membrane fusion. *Biochemistry.* 36:6251–6259.
41. Talbot, W. A., L. X. Zheng, and B. R. Lentz. 1997. Acyl chain unsaturation and vesicle curvature alter outer leaflet packing and promote poly(ethylene glycol)-mediated membrane fusion. *Biochemistry.* 36:5827–5836.
42. Bailey, A. L., and P. R. Cullis. 1997. Liposome fusion. *In* Lipid Polymorphism and Membrane Properties. R. M. Epand, editor. Academic Press, San Diego, CA. 359–373.
43. Karatekin, E., O. Sandre, H. Guitouni, N. Borghi, P. H. Puech, and F. Brochard-Wyart. 2003. Cascades of transient pores in giant vesicles: line tension and transport. *Biophys. J.* 84:1734–1749.
44. Israelachvilli, J. N. 1991. Intermolecular and Surface Forces. Academic Press, London.